Paragenesis and Geochronology of the Nopal I Uranium Deposit, Mexico

[1,6]Fayek, M., [2]Ren, M., [2]Goodell, P., [3]Dobson, P., [4]Saucedo, A., [2]Kelts, A., [5]Utsunomiya, S., [5]Ewing, R.C., [6,1]Riciputi, L.R., [4]Reyes, I.

[1]University of Tennessee, Dept. Earth Planet. Sci., Knoxville, TN 37996, USA
[2]UTEP, Dept. Geological Sciences, El Paso, TX 79968, USA
[3]Lawrence Berkeley National Laboratory, 1 Cyclotron Rd. Berkeley, CA 94720, USA
[4]UACH, Facultad de Ingeniería, Circuíto 1, Nuevo Campus Universitario, Chihuahua, 31302, México
[5]University of Michigan, Dept. Geological Sci., Ann Arbor, MI 48109
[6]Oak Ridge National Laboratory, Oak Ridge, TN 37831, USA

Abstract-*Uranium deposits can, by analogy, provide important information on the long-term performance of radioactive waste forms and radioactive waste repositories. Their complex mineralogy and variable elemental and isotopic compositions can provide important information, provided that analyses are obtained on the scale of several micrometers. Here, we present a structural model of the Nopal I deposit as well as petrography at the nanoscale coupled with preliminary U-Th-Pb ages and O isotopic compositions of uranium-rich minerals obtained by Secondary Ion Mass Spectrometry (SIMS). This multi-technique approach promises to provide "natural system" data on the corrosion rate of uraninite, the natural analogue of spent nuclear fuel.*

I. INTRODUCTION

One of the most challenging aspects of nuclear waste management is the extrapolation of laboratory data collected over short periods of time (hours to years) to the longer periods required in performance assessment calculations [1]. Uranium deposits can provide important information on the performance of radioactive waste forms and radioactive waste repositories [1] because uraninite (UO_{2+X}), the most abundant uranium-bearing mineral in most uranium deposits, is similar in many ways to the UO_2 in spent nuclear fuel [1, 2].

The environment that hosts the Nopal I deposit, Peña Blanca District, Mexico, serves as an important natural laboratory in which to study the oxidation of uraninite and the migration of uranium and other radionuclides over very large spatial (nanometers to kilometers) and temporal scales (thousands to millions of years). However, the fluid evolution of this deposit is complex [3, 4, 5, 6, 7, 8, 9]. In particular, it has been difficult to constrain the timing of interaction between U-rich minerals and post-depositional fluids [3, 4, 6, 7] because the uranium minerals associated with the Nopal I deposit, in particular uraninite, are fine grained (~1-100 μm). These problems are further magnified by the susceptibility of uraninite is susceptible to alteration and radiation damage [10, 11] and by the tendency for the effects from these processes to be manifested at the micrometer scale. To adequately use this ore deposit to assess the degree of actinide and fission product mobility under natural conditions, we must characterize the paragenesis and constrain the timing of fluid-mineral interaction, particularly within the past 1 million years. This information is important for modelling the long-term behaviour of spent nuclear fuel in subsurface repositories.

Characterizing the detailed paragenesis of the Nopal I deposit is crucial because partial oxidation of uraninite, incongruent precipitation of uranyl silicates, and transport of uranium into the geologic environment have been shown to occur in a kinetic series of steps, both experimentally [12] and at the Nopal I deposit [3, 13, 14]. The results of these studies suggest that the rates of uraninite oxidation and formation of secondary uranyl phases exceed the rate of uranyl mineral dissolution and uranium transport out of the mineralized zone. However, these conclusions are based on short duration experiments (weeks) [12], which are difficult to extrapolate to geologic time scales or bulk geochronological methods on selected phases [13,14,15].

Despite the difficulties associated with the study of uraninite in the natural environment [16], its constituents — uranium, lead, oxygen, and thorium — can provide key tools for studying its evolution, provided that analyses are obtained on the scale of several microns. The purpose of this paper is to: (1) refine the current structural and alteration model of the Nopal I to locate and characterize the fast pathways for uranium mobility, (2) re-examine the mineral paragenesis using advanced high-resolution transmission electron microscopic (HRTEM) techniques, and (3) re-examine the chronology of the uranium minerals using state-of-the-art *in situ* techniques such as secondary ion mass spectrometry (SIMS) to obtain realistic uraninite corrosion rates, which

can be used to model spent nuclear fuel corrosion under repository conditions.

II. METHODOLOGY

Petrographic analyses were completed by optical microscopy and electron microscopy of polished thin sections in back-scattered electron mode. Chemical compositions of samples and standards were determined by wavelength-dispersive ion spectroscopy using an automated CAMECA SX50 X-ray microanalyzer operated at 15 keV, a beam diameter of 10 μm, and counting times of 40 s per element. Synthetic $UO_{2.1}$, and ThO_2, grossular, and galena were used as standards for U, Th, Si and Ca, and Pb, respectively. Detection limits of the elements were on the order of 0.1 wt%. The program PAP was used to reduce the data for the various elements. Oxygen contents of uraninite were calculated by stochiometry, assuming an ideal composition of UO_2.

Prior to SIMS analysis, the mounts were re-polished and cleaned to remove the carbon coating, and reflected-light photomaps of the entire mount were made. Although uraninite sufficiently conducts electrons, a ~200 Å thick Au coat was sputter-deposited on the sample mount surface prior to SIMS analysis to ensure a surface conductivity of 5-10 ohms/cm. The mounts were placed in stainless steel sample holders, and the entire assembly was then placed in the SIMS sample lock and held at high vacuum for a minimum of 8 hours prior to the start of analysis.

II.A. Secondary Ionization Mass Spectroscopy (SIMS)

SIMS permits *in situ* measurement of isotopic ratios with a spatial resolution on the scale of a few micrometers by using a focused beam of primary ions impinging on a solid sample surface. The "sputtering" process removes atoms from the polished surface of the specimen. Some of these atoms are ionized and are accelerated as a "secondary" ion beam through a slit and into a mass spectrometer. The relatively high ionization probability for many elements during sputtering allows measurement of isotope ratios for both major and trace elements in nanogram particles, as well as determination of elemental abundances in thin sections and individual grains. Therefore, SIMS is ideal for studying mineralogically complex phases associated with uranium deposits, and considerable effort has been made to develop precise and accurate methods for the analysis of the isotopic ratios by ion microprobe [17, 18].

To successfully apply the SIMS technique to natural analogue studies it is important to obtain and characterize a set of standards. During the measurement process by SIMS, an intrinsic mass dependent bias is introduced, referred to as instrumental mass fractionation (IMF), which depends most strongly on sample characteristics [19]. Therefore, to obtain accurate and precise analyses, chemically and isotopically homogenous mineral standards that are compositionally similar to the unknown are required. Unfortunately, most natural uraninites are chemically and isotopically heterogenous, particularly with regard to elements of interest such as U, Th, Pb, and O [5]. However, we have obtained and characterized two uraninite standards. The first is a synthetic uraninite crystal ($UO_{2.1}$) that was analyzed by conventional methods [20] to determine its oxygen isotopic composition. Multiple measurements (5) gave a $\delta^{18}O$ value of 8.1±0.3‰. Ion microprobe oxygen isotopic analyses of different spots of the UO_2 standard have a standard deviation of ±0.5‰ (1σ). The second standard (TS A uraninite) consists of a single natural uraninite cube (1 cm x 1.5 cm) from a pegmatite in the Topsham Mine, Maine. Chemical and U-Pb isotopic analyses by SIMS of the grain indicate that it is homogenous, with a near-concordant U-Pb age of 314±10 Ma. This suggests that the U-series isotopes have reached secular equilibrium, assuming that the grain remained closed with respect to its U-Th isotope system.

II.B. Transmission Electron Microscopy (TEM) and Scanning Transmission Electron Microscopy (STEM)

TEM samples were prepared from ~30 μm thick polished thin sections that were analyzed by SIMS. Back-scattered electron images were obtained for each sample using a scanning electron microscope (SEM) to locate the exact area analyzed by SIMS. TEM samples of those areas were prepared by drilling 3 mm diameter disks using an ultrasonic drill. The disks were then mechanically thinned by the tripod method to less than 10 μm. The final "thin film" was produced by bombardment with 4.0 kV Ar^+ ions in a Gatan Precision Ion Polishing System. Analytical electron microscopy (AEM) and high-resolution TEM (HRTEM) analysis were obtained using a JEOL 2010F with a point image resolution of 0.23 nm and an accelerating voltage of 200 kV. In obtaining selected area electron diffraction (SAED) patterns, we used a constant size selected aperture so that the size distribution of the uraninite micro-domains could be inferred. An Emispec ES vision 4.0 STEM element mapping system was used to obtain bright field scanning TEM (BF-STEM) distribution maps of Si and U at the nanoscale. The TEM holders were cleaned by plasma (Fischone model C1020) before operation to minimize contamination.

III. RESULTS AND DISCUSSION

III.A.The Nopal I Uranium Deposit

The Nopal I uranium deposit, located within the Peña Blanca district, approximately 50 km north of the city of Chihuahua, Mexico, has been studied extensively by researchers in Mexico, the U.S., and Europe. This deposit is hosted by brecciated Nopal (44 Ma) and Coloradas rhyolitic ash-flow tuffs. These two units overlie the Pozos

conglomerate formation and Cretaceous limestone. The dimensions of the Nopal I deposit at the ground surface are ~25 m by ~70 m, and it extends downward about 90 m; the base of the deposit is about 130 m above the water table.

III.B. Structural Analysis of the Nopal I Deposit

Fieldwork indicates that two dominant fault and fracture systems bound the southwestern and eastern margins of the Nopal I deposit (Fig. 1). The southwestern fault is nearly vertical and strikes 305°. Slickensides on the fault surface dip 20°. The fracture system that bounds the eastern margin of the deposit strikes ~350° and shows very little vertical or horizontal movement. A third fault system is exposed along the +10 level (the top) of the deposit. This fault is nearly horizontal, with a dip of ~20° to the west, and has slickensides that trend 260°. The southwest and east bounding fault and fracture systems occur throughout the Nopal I deposit and appear to have channeled subsequent hydrothermal fluid flow, which resulted in the formation of the breccia pipe that currently hosts the uranium ore. Detailed mapping of the Nopal I deposit shows that brecciation intensifies towards the south, where the west and east bounding fault and fracture systems intersect. Movement along the southwest bounding fault appears to have increased brecciation, which in turn enhanced permeability. As a result, the deposit is zoned, with increasing oxidation towards the southern portion. Other minor and younger fault and fracture systems (e.g., E-W fracture system described by Pearcy et al. [4]) also occur throughout the deposit. These younger fracture systems appear open and permeable to meteoric fluids. The young fractures are lined with secondary U^{6+} minerals where they intersect the main ore body.

III.C. Paragenesis

Detailed petrographic characterization, backscatter electron (BSE) imaging, and selected x-ray maps for the samples from Nopal I high-grade ore zone document a complex uranium mineral paragenesis. There are at least two temporally distinct stages of uranium mineral precipitation. Stage 1 uranium minerals (Ur1; Fig. 2a) precipitated from low-temperature fluids that interacted with existing silicate minerals in the welded tuff. These uranium minerals are mainly associated with quartz (Qtz; Fig. 2a) and can occur along cleavages of feldspar grains. The alteration of Stage 1 uranium minerals resulted in the precipitation of Stage 2 uranium minerals (Fig. 2). Stage 2 uranium minerals are also concentrated along fractures in the tuff. Energy-dispersive spectrometry and x-ray maps suggest that uranophane (Ua), schoepite/dehydrated schoepite (Ds), and weeksite (We) are the dominant Stage 2 uranium minerals (Fig. 2b, c), with minor amounts of Stage 2 uraninite (Ur2; Fig. 2b, d).

Uraninite within the uranium-rich portion of the Pozos conglomerate, which lies nearly 100 m below the main ore body and 30 m above the present day water table, appears to be part of the Stage 2 uranium mineral assemblage. A sample of the Pozos conglomerate was examined using back-scattered electrons (BSE) and HRTEM to characterize the uranium-bearing phases (Fig. 3). BSE imaging as well as elemental mapping of the sample shows that the sample also contains disseminated grains of TiO_2 as well as TiO_2 replacing highly altered sphene. HRTEM analyses identified the phases anatase (TiO_2) and uraninite (UO_2). These preliminary results suggest that anatase is actively sequestering the uranium from the fluids that have interacted with the conglomerate.

III.D. Chronology of the Uranium Minerals and Fluid-Rock Interaction

Three new vertical diamond drill holes (DDHs) were recently drilled at Nopal I. DDH-PB1 with continuous core was drilled through the Nopal I deposit and two additional DDHs were drilled ~50 m on either side of the cored hole. These DDHs terminate ~20 m below the current water table, thus allowing the detection of possible gradients in radionuclide contents resulting from transport from the overlying uranium deposit. Primary uraninite within the main ore body is rare and fine-grained (~50 μm), thus making determination of geochronology of the Nopal I deposit very difficult. Uranium, lead, and oxygen isotopes can be used to study fluid-uraninite interaction, provided that the analyses are obtained on the microscale. Preliminary U-Pb results show that Stage 1 uraninite from the main ore body gives an age of 32±8 Ma (Fig. 2a). U-series analyses of Stage 2 uranium-rich minerals from the main ore body give a range of ages: 3.1±0.5 Ma for uranophane ($Ca(UO_2)_2SiO_3(OH)_25H_2O$), 1.6±0.5 Ma for Stage 2 colloform uraninite, and 85±8 ka for schoepite/dehydrated schoepite (UO_3nH_2O) (Fig. 2b, d). Weeksite/boltwoodite ($K_2(UO_2)_2(SiO_4)_2(H_3O)_2H_2O$) from near the margins of the deposit (Fig. 1) gives an age of 41±5 ka (Fig. 2c).

Uraninite from the uranium-rich portion of the Pozos conglomerate (~475 ppm U) that lies nearly 100 m below the main ore body (~32500 ppm U) and 25 m above the water table (<50 ppb U), gives a U-Pb age that is <1 Ma. This generation of uraninite might be related to the ~1.6 Ma Stage 2 colloform uraninite from the main ore body. However, more analyses are necessary to confirm these results.

Oxygen isotopic analyses show that uraninite from the ore body has a $\delta^{18}O$= -10.8‰, whereas the uraninite within the Pozos conglomerate has a $\delta^{18}O$= -1.5‰. If it is assumed that both uraninites equilibrated with local meteoric water ($\delta^{18}O$= -9‰), then precipitation temperatures calculated using the fractionation factor

equation of Fayek and Kyser [21] are 45–55°C for the uraninite from the ore body and 10–20°C for uraninite hosted by the Pozos conglomerate. These temperatures are consistent with previous studies that calculated stable-isotope precipitation temperatures for clay minerals associated with uraninite at Nopal I [15].

IV. CONCLUSIONS

Previous depositional models of the Nopal I deposit [4, 14], which were based on chemical Pb ages and U-Th ages suggested that deposit formation and alteration occurred as follows: (a) initial uraninite precipitation 8±5 Ma, (b) alteration to U^{6+} phases such as schoepite and weeksite/boltwoodite, (c) a major oxidation event 3.2-3.4 Ma precipitating uranophane, and (d) precipitation of uraniferous Fe-oxyhydroxides (<300 ka), and opal and calcite (54 ka).

Our model explains the localization of the alteration, mineralization, and brecciation of the Nopal I deposit. Weathering resulted in the formation of secondary U^{6+} minerals along fractures, the precipitation of clay minerals, and the development of oxidation zones. Subsequent fault movement along the southwestern margin of the deposit increased brecciation and enhanced permeability, resulting in increased oxidation. U-Th-Pb isotopic ages show that initial uraninite precipitation occurred at 32±8 Ma. A major oxidation event characterized by the precipitation of widespread uranophane did occur at ~3.1 Ma. This event was followed by a reducing event that precipitated a second generation of uraninite at ~1.6 Ma. Subsequently, the deposit was subjected to continued oxidation resulting in the precipitation of schoepite (~85 ka) and weeksite/boltwoodite (~41 ka).

The relationship between uraninite from the Pozos conglomerate and the ~1.6 Ma colloform uraninite from the main ore body is unclear. However, association between the young uraninite and anatase suggests that the Pozos conglomerate formed a natural barrier that sequestered uranium before it reached the water table.

ACKNOWLEDGEMENTS

This work is supported by the Director, Office of Civilian Radioactive Waste Management, Office of Science and Technology and International, of the U.S. Department of Energy under contracts DE-AC02-05740-001-04-30.

REFERENCES

1. J. JANECZEK, R.C. EWING, V.M. OVERSBY, AND L.O. WERME, "Uraninite and UO_2 in spent nuclear fuel: a comparison", *J. Nucl. Mater.*, **238**, 121-130 (1996).
2. R.C. EWING, "Less geology in the geological disposal of nuclear waste", *Science*, **286**, 415-416 (1999).
3. E.C. PEARCY, J.D. PRIKRYL, W.M. MURPHY, AND B.W. LESLIE, "Alteration of uraninite from the Nopal I deposit, Peña Blanca District, Chihuahua, Mexico, compared to degradation of spent nuclear fuel in the proposed U.S. high-level nuclear waste repository at Yucca Mountain, Nevada", *Applied Geochemistry*, **9**: 713-732 (1994).
4. E.C. PEARCY, J.D. PRIKRYL, AND B.W. LESLIE, "Uranium transport through fractured silicic tuff and relative rentention in areas with distinct fracture characteristics", *Applied Geochemistry*, **10**: 685-704 (1995).
5. J.D. PRIKRYL, D.A. PICKET, W.M. MURPHY, AND E.C. PEARCY, "Migration behaviour of naturally occurring radionuclides at the Nopal I uranium deposit, Chihuahua, Mexico", *J. Contam. Hydro.*, **26**: 61-69 (1997).
6. B. GEORGE-ANIEL, J.L. LEROY, AND B. POTY, "Volcanogenic Uranium Mineralizations in the Sierra Peña Blanca District, Chihuahua, Mexico: Three Genetic Models." *Economic Geology*, **86**: 233–248 (1991).
7. B. ANIEL AND J. LEROY, "The reduced uraniferous mineralization associated with the volcanic rocks of the Sierra Peña Blanca (Chihuahua, Mexico)", *American Mineralogist*, **70**:1290-1297 (1985).
8. D.A. PICKETT, AND W.M. MURPHY, "Isotopic Constraints on Radionuclide Transport at Pena Blanca." *Seventh EC Natural Analogue Working Group Meeting: Proceedings of an International Workshop held in Stein am Rhein, Switzerland from 28 to 30 October 1996. von Maravic, H. and Smellie, J., eds. EUR 17851 EN. Pages 113-122. Luxembourg, Luxembourg: Office for Official Publications of the European Communities* (1997).
9. E.C. PEARCY, J.D. PRIKRYL, W.M. MURPHY, AND B.W. LESLIE, Uranium Mineralogy of the Nopal I Natural Analog Site, Chihuahua, Mexico. *CNWRA 93-012. San Antonio, Texas: Center for Nuclear Waste Regulatory Analyses* (1993).
10. J. JANECZEK AND R.C. EWING, "Mechanisms of lead release from uraninite in natural fission reactors in Gabon", *Geochim. Cosmochim. Acta*, **59**, 1917-1931 (1995).
11. T.G. KOTZER AND T.K. KYSER, "Petrogenesis of the Proterozoic Athabasca Basin, northern Saskatchewan, Canada, and its relation to diagenesis, hydrothermal uranium mineralization and paleohydrogeology", *Chem. Geol.*, **120**, 45-89 (1995).
12. D.J. WRONKIEWICZ AND E.C. BUCK, "Uranium

mineralogy and the geologic disposal of spent nuclear fuel", in *Uranium: Mineralogy, Geochemistry, and the Environment, (eds. P.C. Burns and R. Finch), Min. Soc. Proc.*, **38**; 475-497 (1999).

13. W.M. MURPHY, "Source–term constraints for the proposed repository at Yucca Mountain, Nevada, derived from the natural analog at Peña Blanca, Mexico", *Mat. Res. Symp. Proc.*, **257**: 521-527 (1992).
14. W.M. MURPHY, "Natural analogues and performance assessment for geologic disposal of nuclear waste", *Mat. Res. Symp. Proc.*, **608**: 533-544 (2000).
15. P. ILDEFONSE, P. AGRINIER, AND J.P. MULLER, "Crystal-chemistry and isotope geochemistry of alteration associated with the uranium Nopal I deposit, Chihuahua, Mexico", *Chemical Geology*, **84**: 371-372 (1990).
16. R.J. FINCH AND R.C. EWING, "Corrosion of uraninite under oxidizing conditions", *J. Nucl. Mater.*, **190**: 133-156 (1992).
17. M. FAYEK, T.K. KYSER, AND L.R. RICIPUTI, "U and Pb isotope analysis of uranium minerals by ion-microprobe and the geochronology of the McArthur River and Sue Zone uranium deposits, Saskatchewan Canada", *Can. Min.*, **40**: 1717-1733 (2002).
18. M. FAYEK, T.M. HARRISON, R.C. EWING, M. GROVE, AND C.D. COATH, "O and Pb isotopic analyses of uranium minerals by ion microprobe and U-Pb ages from the Cigar Lake Deposit", *Chem. Geol.*, **185**: 205-225 (2002).
19. N. SHIMIZU AND S.R. HART, "Applications of the ion-microprobe to geochemistry and cosmochemistry", *Annu. Rev. Earth Planet. Sci*., **10**, 483-526 (1982).
20. R. CLAYTON AND T.K. MAYEDA, "The use of bromine pentafluoride in the extraction of oxygen from oxides and silicates for isotopic analysis", Geochim. Cosmochim. Acta, **27**: 43-52 (1963).
21. M. FAYEK AND T.K. KYSER, "Low temperature isotopic fractionation in the uraninite-UO_3-CO_2-H_2O system", *Geochim. Cosmochim.*, **64**: 2185-2197 (2000).
22. I. A. REYES-CORTÉS, "Geologic Studies in the Sierra de Peña Blanca, Chihuahua, Mexico", unpublished Ph.D. thesis, University of Texas, El Paso: 344p. (1997).

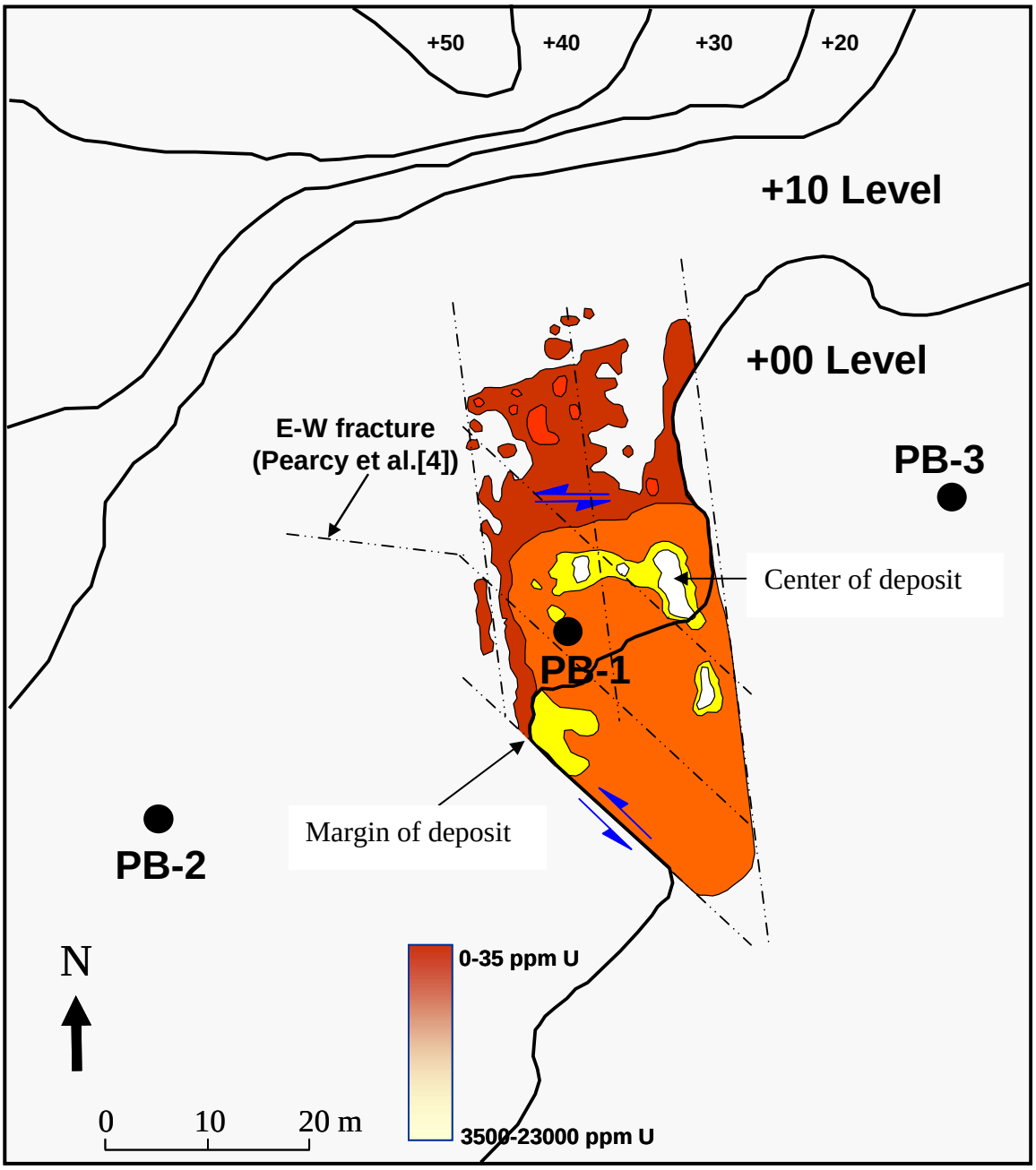

Figure 1. Plan view of the Nopal I deposit showing the uranium rich zones, the location of the three wells (PB-1, 2, 3), and the major fracture/fault systems that define the margins of the deposit (dotted lines). Also shown is the E-W fracture system describe in Pearcy et al. [4]. Modified from Reyes-Cortés [22].

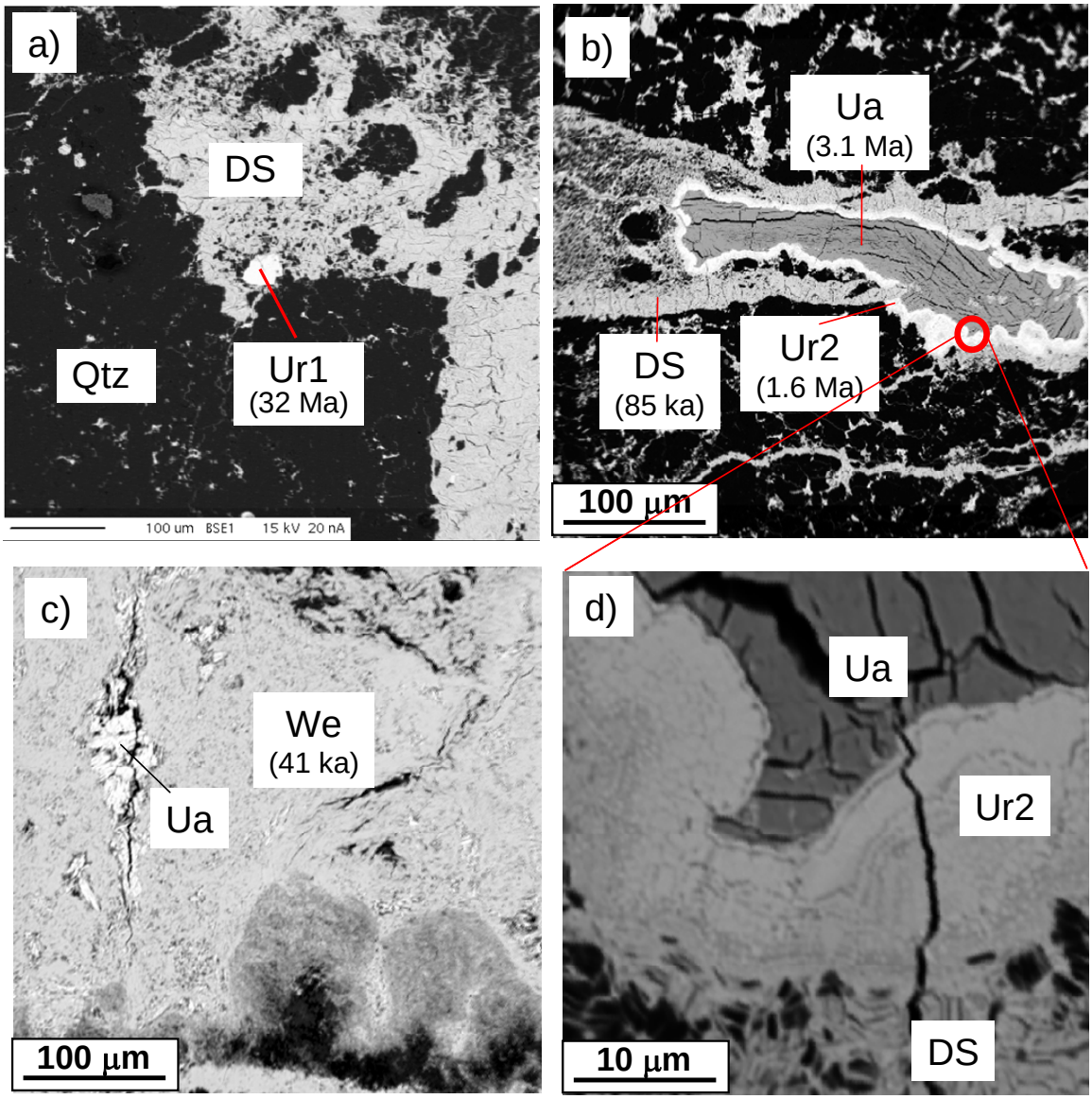

Figure 2. Back-scattered electron images of representative surface outcrop samples and samples from the adit collected from a) the central portion of the deposit showing 32 Ma Stage 1 uraninite (Ur1), quartz (Qtz), and Stage 2 schoepite/dehydrated schoepite (DS); b) the central portion of the deposit showing Stage 2 uranium minerals; 3.1 Ma uranophane (Ua), 1.6 Ma uraninite (Ur2), and 85 ka schoepite/dehydrated schoepite (DS); c) near the margins of the deposit showing Stage 2 uranophane (Ua) and 41 ka weeksite/ boltwoodite (We); and d) high-resolution image of the area circled in red in (b) showing the colloform texture of Stage 2 uraninite (Ur2).

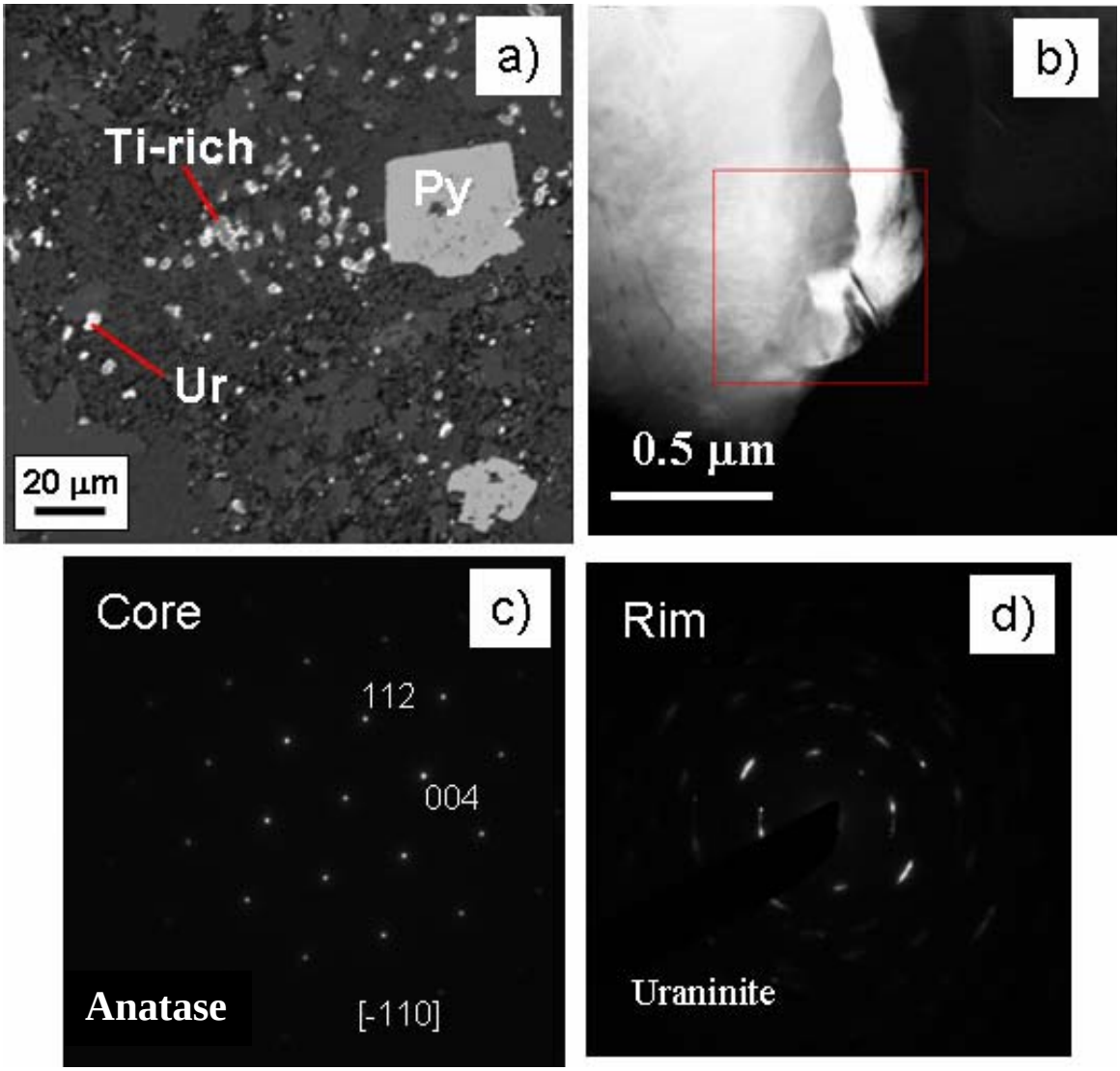

Figure 3. a) Back-scattered electron image of the Pozos conglomerate showing the uraninite (Ur) associated with Ti-rich minerals and pyrite (Py); b) Scanning transmission electron microscope (STEM) image of a U-Ti-rich grain from the Pozos conglomerate. Electron dispersive patterns (c and d) obtained from within the area outlined by the red box in (b) show that the core and rim are consistent with anatase and uraninite, respectively.